



HAL
open science

Dilute and concentrated phases of vesicles at thermal equilibrium

P. Hervé, D. Roux, A.-M. Bellocq, F. Nallet, T. Gulik-Krzywicki

► **To cite this version:**

P. Hervé, D. Roux, A.-M. Bellocq, F. Nallet, T. Gulik-Krzywicki. Dilute and concentrated phases of vesicles at thermal equilibrium. *Journal de Physique II*, 1993, 3 (8), pp.1255-1270. 10.1051/jp2:1993196 . jpa-00247902

HAL Id: jpa-00247902

<https://hal.science/jpa-00247902>

Submitted on 4 Feb 2008

HAL is a multi-disciplinary open access archive for the deposit and dissemination of scientific research documents, whether they are published or not. The documents may come from teaching and research institutions in France or abroad, or from public or private research centers.

L'archive ouverte pluridisciplinaire **HAL**, est destinée au dépôt et à la diffusion de documents scientifiques de niveau recherche, publiés ou non, émanant des établissements d'enseignement et de recherche français ou étrangers, des laboratoires publics ou privés.

Classification
Physics Abstracts
82.70 — 61.25

Dilute and concentrated phases of vesicles at thermal equilibrium

P. Hervé (^{1,*}), D. Roux (¹), A.-M. Bellocq (¹), F. Nallet (¹) and T. Gulik-Krzywicki (²)

(¹) Centre de recherche Paul-Pascal, CNRS, avenue du Docteur-Schweitzer, 33600 Pessac, France

(²) Centre de génétique moléculaire, CNRS, 91190 Gif-sur-Yvette, France

(Received 15 March 1993, accepted in final form 7 May 1993)

Abstract. — A quaternary system made of an ionic surfactant (SDS), octanol, water and sodium chloride has been investigated. We present experimental results that demonstrate the existence of a phase of vesicles at thermal equilibrium. We show that vesicles can be prepared both in a dilute regime leading to an isotropic liquid phase of low viscosity and in a concentrated regime leading to a phase of close packed vesicles (probably multilayered) exhibiting high viscosity and viscoelasticity.

Introduction.

Surfactants in solutions have been extensively studied in the last decades : they are fascinating examples of self-assembling systems and have motivated a lot of theoretical and experimental developments [1]. Along with many other structures, surfactants may aggregate into two-dimensional objects : films (monolayers) or membranes (bilayers). The membranes formed by the association of surfactant molecules have many ways to fill up space, leading to various structures. At low surfactant concentration, one can find either liquid crystalline phases of membranes stacked into a lamellar structure [2] or isotropic liquid phases of randomly connected membranes called sponge phases [3, 4]. One can show [5] that upon dilution, sponge phases undergo a phase transition, of either first [3-6] or second order [7], toward disconnected pieces of membranes that in the dilute regime are composed of isolated vesicles. Up to now the systems studied (which can be characterized by very flexible membranes) have exhibited only a very narrow range of stability for the vesicle phase. However, in other systems (that we believe to be made of more rigid membranes), stable phases of vesicles have been located [8-10].

The existence of thermodynamically stable phases of vesicles has been the subject of a large debate in the literature [11]. It is now well demonstrated experimentally that such a system

(*) *Present address* : L'Oréal, 1 avenue Eugène-Schueller, B.P. 22, 93601 Aulnay-sous-Bois Cedex, France.

exists [8-13]. From a theoretical view point, one can understand that the stability of vesicles is either due to the entropy of mixing [14] or helped by some more specific interactions [15].

We present in this paper a series of experimental results obtained with a quaternary system showing that a phase of stable vesicles exists at thermal equilibrium. The most interesting feature of this phase is that vesicles exist both in dilute and concentrated regimes. Indeed, as explained in what follows, a concentration threshold exists (that we call c^* by analogy to the appearance of the semi-dilute regime in polymer solutions) above which the vesicles are close packed.

Phase diagram.

The system studied is made of four components : water, sodium chloride, octanol and sodium dodecylsulfate (SDS). We present in figure 1 a schematic cut of the phase diagram at constant salt over water ratio (NaCl concentration is 20 g l^{-1}). We have focussed on the dilute part of the phase diagram, corresponding to the water/NaCl corner. Four phases can be described : a micellar phase (L_1), a lamellar phase (L_α), a sponge phase (L_3) and a isotropic phase (L_4), with a very narrow range in alcohol concentration, sandwiched between L_1 and L_α . As already observed in similar systems [3] the phase boundaries are straight lines, directed toward the water/salt corner, therefore corresponding to a constant octanol over SDS ratio (for the L_4 phase, octanol/SDS = 0.3 in weight). We may thus consider that any linear path located inside a one-phase domain and pointing toward the water/salt corner corresponds to a dilution line at constant membrane composition. In the following, all the compositions will be given as *surfactant* weight fraction ; the *membrane* volume fraction is equal to twice the surfactant weight fraction.

The analysis of the structures of the lamellar and sponge phases shows that both systems are made of bilayers, containing all the SDS and the octanol, with thickness 24 \AA [16]. We have

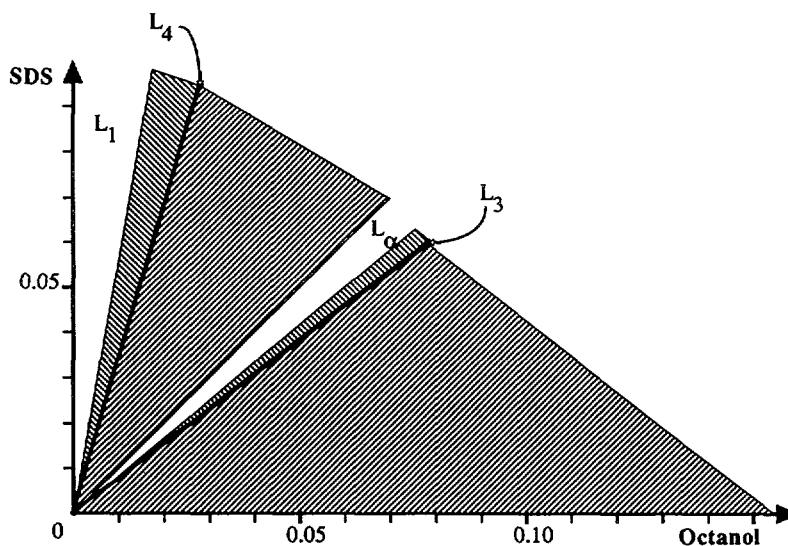


Fig. 1. — Schematic view of the dilute part of the phase diagram of the SDS/octanol/water/NaCl system ; the concentration of NaCl in water is fixed : 20 g/l . Four one-phase regions are shown, separated with first order transitions (hatched regions) : L_1 is a micellar phase, L_α is a lamellar phase (lyotropic smectic A) ; L_3 and L_4 , both with a very narrow range in alcohol concentration, are respectively the sponge phase and the vesicle phase.

not analysed in detail the L_1 phase but its basic properties (viscosity, conductivity, light scattering) indicate that it is composed of small objects (probably micelles).

Viscosity measurements.

One of the most striking properties of the L_4 phase is its viscosity : it evolves a lot, as a function of surfactant concentration, from a low viscous liquid at low surfactant concentration to a very viscous phase at higher surfactant concentration. This large increase in viscosity happens around 4 % in surfactant weight fraction and is easily observable when preparing samples. In order to investigate this behaviour more accurately, we have measured the viscosity as a function of the shear rate for a series of samples, along a dilution line. The experiments have been performed on a constant stress rheometer (CSL 100, Carri-Med, UK) covering a large range of shear rates (0.1 to 100 s^{-1}). Figure 2 presents the stress as a function of the shear rate for a series of samples. At low surfactant content (below a characteristic

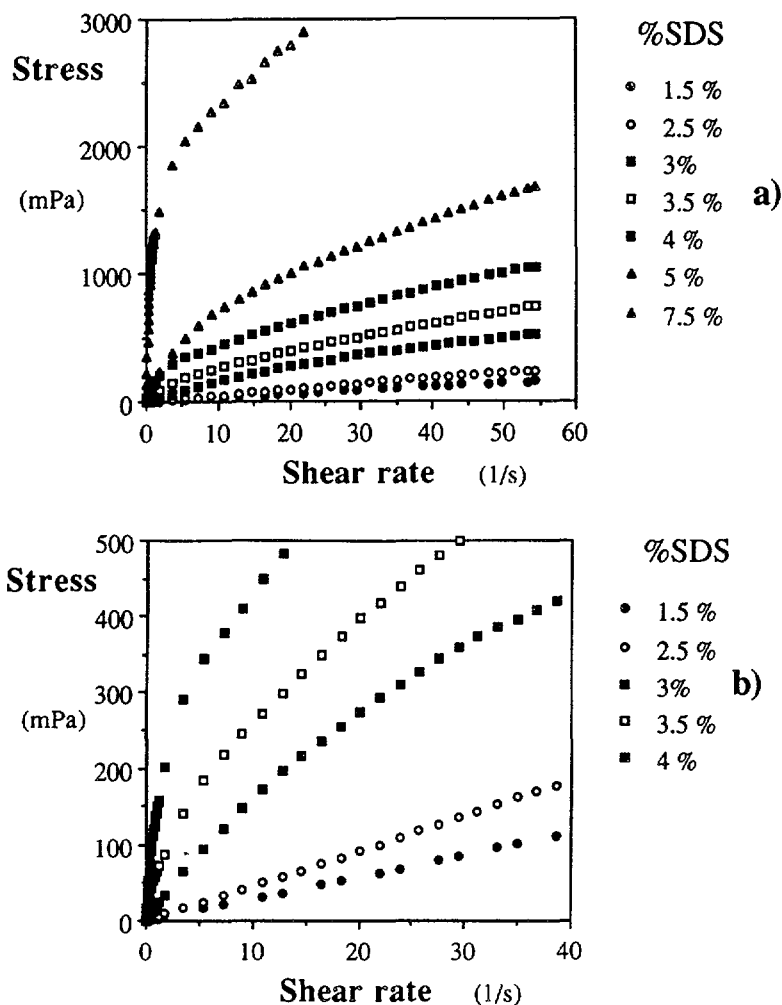


Fig. 2. — a) Plot of the stress as a function of the shear rate for a series of samples prepared in the L_4 phase at different SDS weight fractions. b) Enlargement of the low stress region in the previous plot.

surfactant weight fraction $c^* \approx 3.6\%$) the L_4 phase displays a Newtonian behaviour, i.e. stress is proportional to shear rate with a constant viscosity (see Fig. 3a). Above c^* , a shear thinning behaviour is observed: the viscosity decreases when the shear rate is increased. Figure 3b is a plot of the viscosity, extrapolated at zero shear as a function of the surfactant weight fraction c . It is clear that below c^* the viscosity increases slowly with c , from the viscosity of the solvent to a few times this value, whereas above c^* there is a very much stronger increase (up to several thousand times the solvent viscosity).

Conductivity.

Conductivity measurements have also been performed on the same system. In figure 4 we compare conductivities measured in the L_1 and L_4 phases. As surfactant concentration

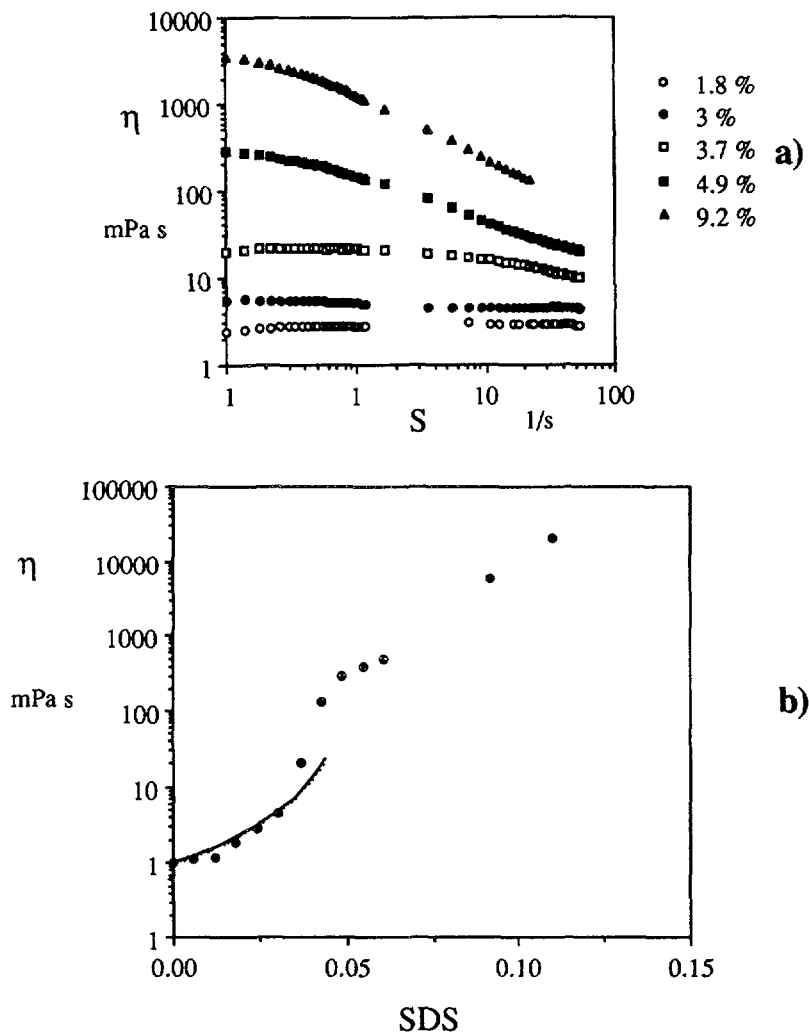


Fig. 3. — Values of the viscosities for a series of samples in the L_4 phase. Viscosities result from the measurements displayed in figure 2. Figure 3a presents the behaviour of the viscosity as a function of the shear rate and figure 3b the viscosity extrapolated at zero shear rate as a function of the surfactant weight fraction.

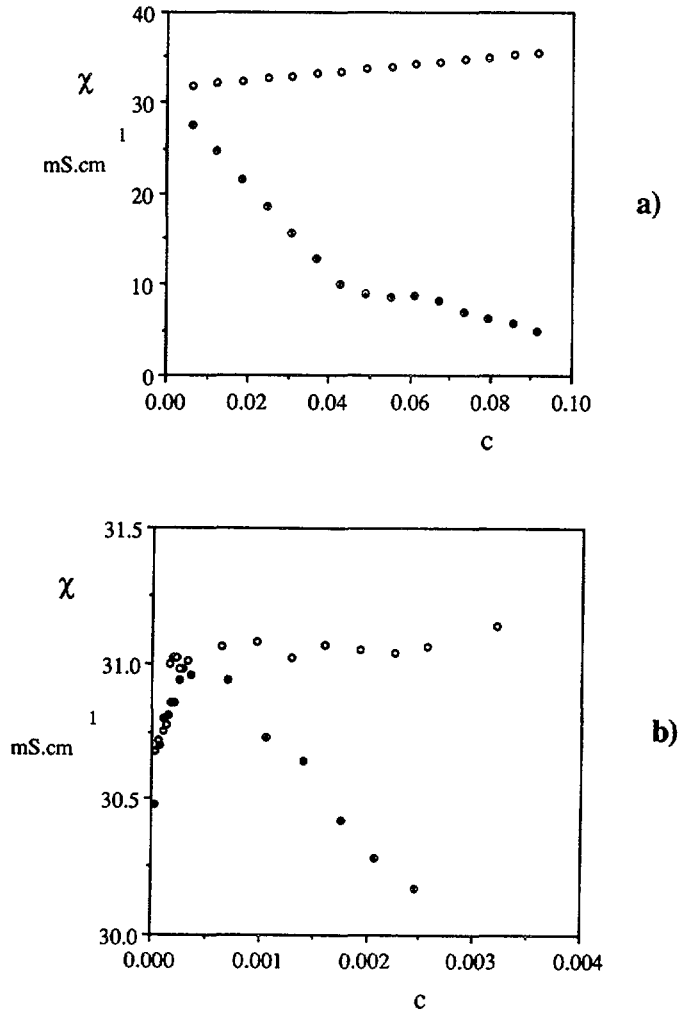


Fig. 4. — Conductivity measurements in the L_4 (dots) and L_1 (open circles) phases as a function of the surfactant weight fraction. The difference of behaviour is very striking and can be interpreted as due to the encapsulation of a large part of the volume in the vesicle phase (L_4).

increases, the conductivity of the micellar phase L_1 remains practically constant at a value very close to the water/salt conductivity (see Fig. 4a). The slight increase observed is due to the addition of surfactant (SDS is an ionic surfactant) either as micelles (above the Critical Micellar Concentration : CMC) or as free molecules (below the CMC). The break in slope, observed at a very low concentration is the usual signature of the CMC (see Fig. 4b, CMC = 0.03 % in water/NaCl 20 g l⁻¹) [17]: owing to their greater mobility, free surfactant molecules carry current more efficiently than the much bigger micelles.

As in the case of the micellar phase L_1 , the initial conductivity increase in the L_4 phase is due to free surfactants. Then large objects are formed (as checked independently by light scattering), leading to a conductivity *maximum*. By analogy with the L_1 phase and anticipating the interpretation we call the location of this maximum the Critical Vesicle Concentration (CVC). Above the CVC, the L_4 conductivity departs markedly from the L_1 behaviour : indeed a very significant decrease, approximately linear in c , is first observed,

followed by a slower decrease above about c^* (Fig. 3a). The ratio between the conductivities in the L_4 and L_1 phases varies from 1 at very low concentrations (below the CMC) to less than 0.3 at high concentrations (above c^*). Since both phases are made with the same components with only a slightly different octanol/SDS ratio, the difference in behaviour is very striking. For comparison, the obstruction obtained by random bilayers (L_3 phase) leads to a ratio of the order of 0.6 [3, 6, 18].

Freeze fracture.

In order to achieve the best preservation of the sample structure upon cryofixation, we replaced water with a water-glycerol (33 % in volume) solution and checked that this replacement did not modify the phase diagram. In fact, from a systematic study of the effect of co-surfactant on the stability of vesicle phases, we know that the basic phases and phase diagram topology are preserved with glycerol when using an alcohol one carbon longer [19]. For this reason, we present here pictures which have been obtained with nonanol instead of octanol. The topology of the pseudo-ternary nonanol-SDS-water (containing 33 % of glycerol and 20 g/l NaCl) was shown to be qualitatively identical to the octanol/SDS/ brine and quantitatively very close to it (typical boundaries are moved less than 20 %).

For freeze fracture electron microscopy, a thin layer of the sample (20-30 μm thick) was placed on a thin copper holder and then rapidly quenched in liquid propane. The frozen sample was then fractured at -125°C , in a vacuum better than 10^{-6} Torr, with a liquid-nitrogen-cooled knife in a Balzers 301 freeze etching unit. The replication was done using unidirectional shadowing, at an angle of 35° , with platinum-carbon, 1 to 1.5 nm of mean metal deposit. The replicas were washed with organic solvents and distilled water, and were observed in a Philips 301 electron microscope.

Figure 5 presents two pictures obtained with samples at surfactant weight fractions respectively equal to 2 % and 5 % (below and just above c^* for the nonanol/glycerol system). First of all, the pictures clearly show the existence of a polydisperse population of vesicles with sizes (radii) ranging from less than 100 \AA to more than 2 000 \AA . The average radius R_{av} is easily obtained (the size distribution also, as discussed later); we get: $R_{\text{av}} = 550 \text{ \AA}$ for $c = 2 \%$ and $R_{\text{av}} = 400 \text{ \AA}$ for $c = 5 \%$. We can also stress that the vesicles, even if they look spherical on average are very often slightly deformed indicating that they are not under tension, unlike the vesicles which are prepared by either sonication or extrusion.

Dynamic light scattering.

Dynamic light scattering experiments have been performed, in order to determine the characteristic size of the structure. Below the CVC, no objects with sizes larger than a few \AA (molecular size) can be observed. Above the CVC and below c^* we get a practically monoexponential signal, therefore characterized by a single characteristic frequency. Figure 6 shows this frequency as a function of the square of the scattering wave vector q , for a sample with $c = 1 \%$. For all samples in this concentration range, the frequency is proportional to q^2 [20], where the proportionality constant (a diffusion coefficient D) is basically constant until c^* is reached. Above c^* , it is very difficult to extract any quantitative results from light scattering: the signal is no longer monoexponential and typical frequencies are very low (of the order of a few s^{-1}). From the diffusion coefficient ($D = 3 \times 10^{-12} \text{ m}^2 \text{ s}^{-1}$) obtained below c^* and using Stokes-Einstein law, one can extract a characteristic radius of the scattering objects ($R = k_B T / 6 \pi \eta D$); we get: $R = 700 \text{ \AA} \pm 100 \text{ \AA}$.

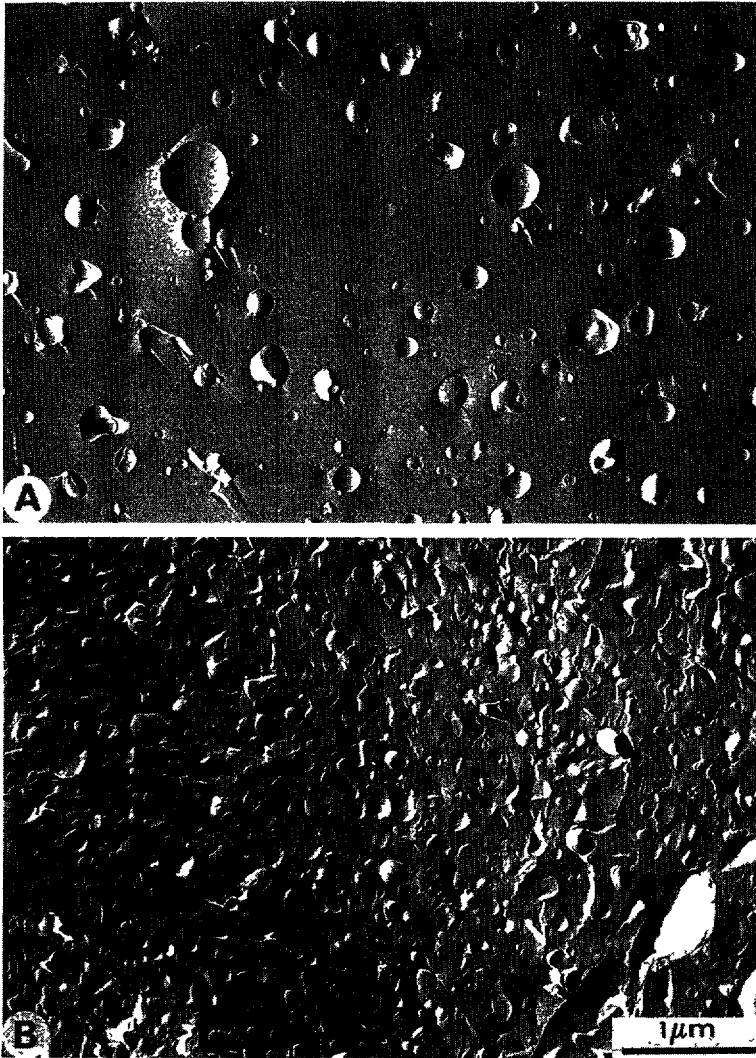


Fig. 5. — Freeze-fracture electron micrographs of the L_4 phase prepared with nonanol/SDS/water/NaCl (20 g/l) and 33 % of glycerol. a) Corresponds to 2 % of surfactant and b) to 5 % (just above c^*). Notice the presence of heterogeneous population of vesicles, which are more concentrated and smaller (in average) for higher surfactant concentration.

Theoretical model for dilute vesicles.

We may understand quantitatively the stability and properties of the dilute vesicle phase with the following, simple model : we assume, as is classically done [14], that vesicles are at thermal equilibrium. Their size and size distribution thus result from the competition between entropic and elastic contributions to the vesicle free energy. Within the framework of the membrane elasticity theory [21] we have a bending energy E of a piece of membrane of the following form :

$$E = \int \left[\frac{1}{2} \kappa \left(\frac{1}{R_1} + \frac{1}{R_2} \right)^2 + \bar{\kappa} \frac{1}{R_1 R_2} \right] dS \quad (1)$$

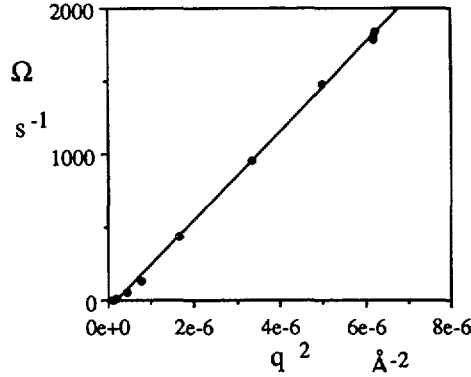


Fig. 6. — Characteristic frequency of the intensity-intensity correlation function obtained by dynamic light scattering as a function of the square of the wave vector, for a sample containing 1 % of surfactant weight fraction. The best fit corresponds to a diffusion coefficient equals to $3 \times 10^{-12} \text{ m}^2 \text{ s}^{-1}$

where R_i are the principal radii of curvature of the membrane and κ and $\bar{\kappa}$ are respectively the average and Gaussian bending constants. Integrating equation (1) and assuming a spherical shape, it is easy to calculate the curvature energy of one vesicle :

$$E_{\text{ves}} = 4 \pi (2 \kappa + \bar{\kappa}) . \quad (2)$$

With the assumption that vesicles are non-interacting objects, the entropic contribution to the free energy reduces to the entropy of mixing. Then, as has already been shown [14] the fact that the elastic energy of a vesicle is independent of its size allows for a *finite* equilibrium size, function of the surfactant concentration (the aggregation number i varies in the same way as the square root of the surfactant concentration c). This is rather similar to the problem of the growth of cylindrical micelles [14]. However, as also noticed previously, the elastic constants are renormalized by thermal fluctuations [22, 23]. This makes the elastic energy of a vesicle (Eq. (2)) weakly size dependent. As suggested, this renormalization should modify both the size and size distribution [24]. We here derive a general result for the equilibrium size and polydispersity, within this framework.

The renormalization of the elastic constants is a function of both short and long wavelength cutoffs, which can be taken respectively as the bilayer thickness δ and the vesicle radius R [22, 23] :

$$\kappa = \kappa_0 - \alpha \frac{k_B T}{4 \pi} \ln \left[\frac{R}{\delta} \right] \quad (3a)$$

$$\bar{\kappa} = \bar{\kappa}_0 + \bar{\alpha} \frac{k_B T}{4 \pi} \ln \left[\frac{R}{\delta} \right] \quad (3b)$$

α and $\bar{\alpha}$ are numerical coefficients equal to 3 and 10/3, respectively [23]. When combined with the ideal mixing entropy (see Appendix), this renormalization effect leads to thermodynamic quantities (average sizes, volume fraction occupied by vesicles, etc.) slightly different from the classical result [14]. In particular, we get the volume fraction X_i of the surfactant molecules aggregated in vesicles of size (aggregation number) i :

$$X_i = i^\gamma \left(1 - \left(\frac{\gamma! e^{-\frac{E_0}{kT}}}{c} \right)^{1/(\gamma+1)} \right)^i e^{-\frac{E_0}{kT}} \quad (4)$$

with $\gamma = 1 + \alpha - \bar{\alpha}/2 = 7/3$ and $E_0 = 4 \pi (2 \kappa_0 + \bar{\kappa}_0)$.

An average radius is easily deduced from this size distribution function :

$$R_{av} = \frac{\sum_{i=1}^{\infty} r_i \frac{X_i}{i}}{\sum_{i=1}^{\infty} \frac{X_i}{i}} \quad (5a)$$

with r_i the radius of type i vesicles. It may be computed as (see Appendix) :

$$R_{av} = 2.47 r_0 (ac)^{\frac{1}{2(\gamma+1)}} \quad (5b)$$

with $r_0 = (\Sigma_s/8 \pi)^{1/2} \approx 1 \text{ \AA}$ (for an area per polar head $\Sigma_s = 24 \text{ \AA}^2$) and $a = \exp(E_0/k_B T)$. The average radius is a weak function of the surfactant concentration :

$$R_{av} \propto c^{3/20} \quad (6)$$

The volume fraction ϕ occupied by the vesicles is :

$$\phi = \sum_{i=1}^{\infty} \frac{4}{3} \pi r_i^3 \frac{X_i}{i v_s} \quad (7a)$$

(with v_s the volume of one surfactant molecule) and given by (see Appendix) :

$$\phi = 1.58 \frac{r_0}{3 \delta} (ac)^{\frac{1}{2(\gamma+1)}} c . \quad (7b)$$

It increases a little bit faster than linearly (exponent 1.15) due to the slight increase of the average size with the surfactant concentration.

Discussion.

The theoretical predictions for a dilute vesicle phase are compared to the conductivity and other data. The conductivity of a phase of vesicles occupying a volume fraction ϕ can be calculated by taking two effects into account. Firstly, as part of the brine volume is encapsulated inside vesicles, a volume fraction exactly equal to ϕ does not contribute to the low frequency conductivity. Consequently, the effective conductivity is obtained only from the water situated outside vesicles, in relative amounts $(1 - \phi)$. In addition to this main effect, a tortuosity due to the presence of insulating spheres has to be introduced. This obstruction factor has been calculated to be $1/(1 + \phi/2)$ [25]. The conductivity χ of a phase of vesicles is therefore given by :

$$\frac{\chi}{\chi_0} = \frac{1 - \phi}{1 + \phi/2} \quad (8)$$

where χ_0 is the conductivity of the brine (we have neglected the extra conductivity brought by the SDS counterions). Inverting equation (8) we get the volume fraction ϕ of vesicles as a function of the conductivity ratio χ/χ_0 .

$$\phi = \frac{1 - \chi/\chi_0}{1 + \chi/2 \chi_0} \quad (9)$$

Figure 7 shows the volume fraction of vesicles, calculated from the conductivity data and equation (9) as a function of the surfactant weight fraction c . There is first an initial increase of the volume fraction of vesicles, apparently linear in c ; then at c^* there is a clear break in the curve showing a levelling off of the volume fraction. Note that the close packing regime corresponds to a value for ϕ of the order of 60 %. In order to examine the concentration dependence more closely, we plot with double logarithmic axes the volume fraction as a function of the membrane concentration (we have used c -CVC for the horizontal axis), keeping only data corresponding to concentrations lower than c^* (3.6 %), i.e. in the dilute regime. An exponent slightly larger than one (1.05 ± 0.05) can be extracted from the data, see figure 8.

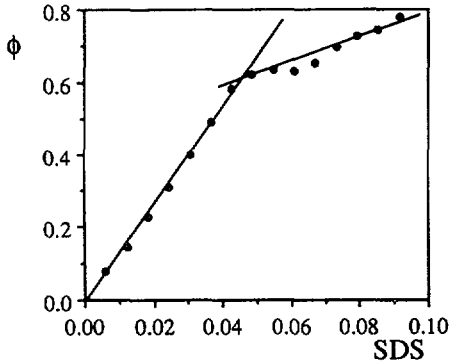


Fig. 7.

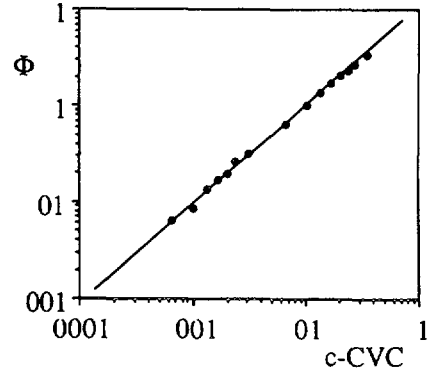


Fig. 8.

Fig. 7. — Volume fraction extracted from the conductivity measurements using equation (8). The approximate linear behaviour corresponds to the dilute regime and the break at 4 % corresponds to the close packing regime (concentrated).

Fig. 8. — Double logarithmic plot of the volume fraction extracted using equation (8) in the dilute regime as a function of the surfactant weight fraction (c -CVC). The best fit corresponds to an exponent slightly larger than 1 (1.05).

This value is more compatible with the exponent theoretically expected, taking into account renormalization of the elastic constants (1.15) than with the classical expectation (1.25) [14].

We may also estimate the value of E_0 , using both the average size as obtained from light scattering and the amplitude of the volume fraction variation. Using equations (5) and (7), we found $E_0 \approx 57 kT$ in both cases. For this system, we have independently measured the value of κ using light scattering on oriented samples in the lamellar phase [16] ($\kappa_0 = 4 k_B T$). Besides, it has also been shown, both theoretically and experimentally that κ is not sensitive to the alcohol concentration (when the alcohol/surfactant ratio is larger than 1 molecule of alcohol per surfactant) [26]. Consequently, one can estimate the value of $\bar{\kappa}_0$. we found $\bar{\kappa}_0 = -3.4 k_B T$.

Using the vesicle volume fraction ϕ obtained from conductivity data, equation (9), one can now analyze the viscosity of the L_4 phase, in the dilute ($\phi < \phi^*$) regime. As a model, we take the viscosity of a hard sphere suspension [27] :

$$\eta = \eta_s \left(1 - \frac{\phi}{\phi^*} \right)^{-2} \quad (10)$$

with η_s being the solvent viscosity and ϕ^* the close packing volume fraction ($\phi^* = 0.63$).

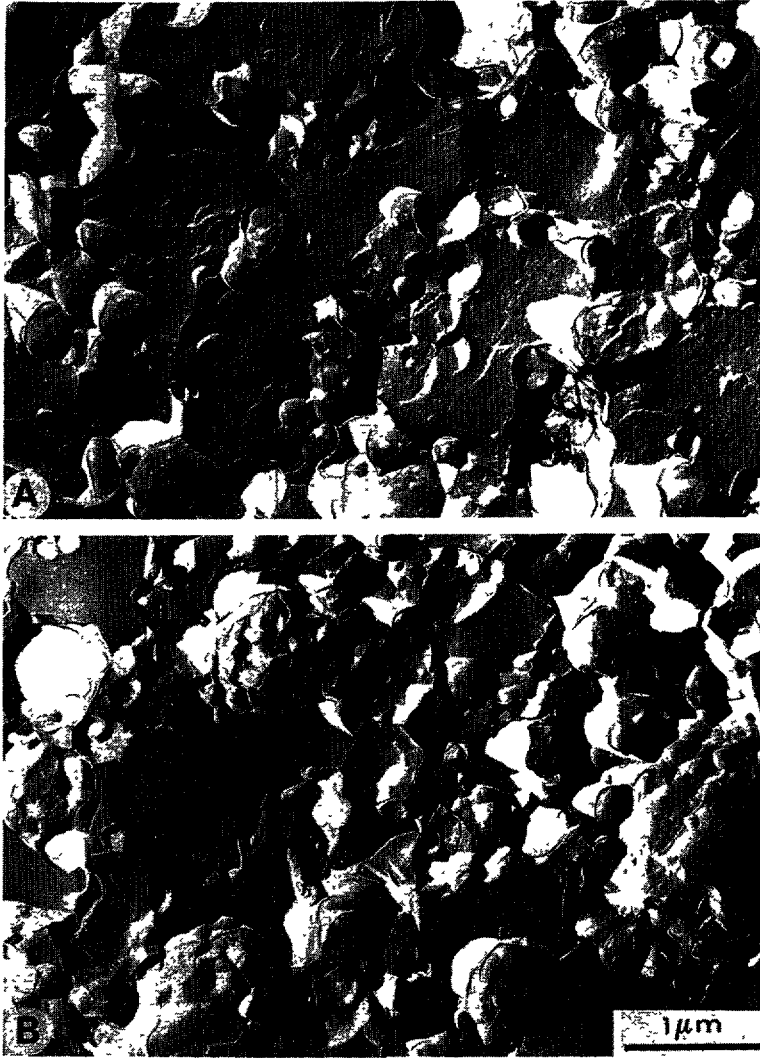


Fig. 9. — Two different regions a) and b) of the freeze-fracture electron micrograph for a sample, prepared with nonanol/SDS/water (33 % glycerol)/NaCl (20 g/l) in the L_4 region of the phase diagram. The surfactant weight fraction is 9 %. Notice in a) the presence of large multilamellar vesicles.

The solid line in figure 3b is obtained from equation (10). It is clear that in the dilute regime ($c < c^*$), the viscosity is well interpreted by the hard sphere model. When the vesicle volume fraction becomes of the order of the close packing value, this is no longer true and the viscosity increases much faster.

As we have seen on the electron microscopy pictures an assembly of vesicles still exists, even when the close packing value is reached. The other experiments indicate that beyond close packing there is a crossover to another regime. For instance, the conductivity levels off, indicating a saturation of the volume fraction occupied by the vesicles ; the phase becomes viscoelastic with relaxation times clearly longer than in the so-called dilute regime. What is the structure above c^* ? Several hypotheses can be made : one can think of a shrinking of the

vesicles ; indeed, one can keep the *vesicle* volume fraction practically constant and still increase the *surfactant* weight fraction by making the vesicles smaller in size. One can also think of going to multilamellar vesicles [28] that will preserve the growing of the vesicles by accommodating more surfactant. One may also think of a deformation of the vesicles to elongated objects (disk-like or rod-like) : this will obviously lead to a nematic state. Experimentally the phase which depolarizes light is not a nematic (no texture characteristic of this type of organization) ; we may consequently eliminate this hypothesis.

We are presently investigating the structure of the concentrated regime with neutron scattering [19]. However, freeze fracture experiments already give an idea of what happens. Figure 9 shows freeze fracture images of a sample above c^* . The objects seen are much bigger (the scale is the same as in Fig. 5) and most of them probably correspond to multilamellar vesicles. Recently, Simons and Cates [28] have theoretically proposed that effectively such a phase may exist in an intermediate regime between the (unilamellar) vesicle phase and the lamellar phase. In the first step, when vesicles become more concentrated these authors find that the size distribution narrows ; this is due to cutting off the larger sizes. It is striking to check this prediction by comparing the distributions obtained from the electron micrographs at $c = 2\%$ with the distribution at 5% (just above c^*). Indeed, figure 10 shows the effect of approaching the close packing on the distribution : the average size is lowered, as expected, to keep the volume fraction of vesicles constant. The distributions have been obtained using a deconvolution procedure [32] allowing a three-dimensional distribution from a two-dimensional cut. The solid line corresponds to the distribution calculated theoretically from equation (4). The decay of the average vesicle size seems to be achieved not by moving all the distribution to smaller values of R but rather by cutting off the large sizes. In the Simons and Cates description, this behaviour would lead to a crystal phase of monodisperse vesicles. In fact to preserve some entropic gain, the system prefers to go to multilayer vesicles rather than to continue to shrink the unilamellar vesicles. This second step could correspond to the break that is observed in the viscosity curve above c^* (Fig. 3).

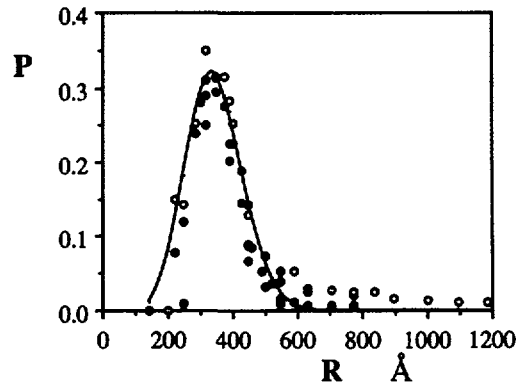


Fig. 10. — Size distribution functions, measured in figures 5a and b. The open circles (resp. the dots) correspond to 2% (resp. 5%) in surfactant weight fraction. The deconvolution has been obtained following the algorithm of reference [32]. It is clear that when the most probable size does not vary, the large sizes disappear in the most concentrated sample.

Conclusions.

Using different techniques such as conductivity, rheometry, light scattering and freeze fracture electron microscopy we have shown that a phase of vesicles at thermal equilibrium exists in a quaternary system. Two regimes can be described. The first one corresponds to a dilute phase of vesicles, with the properties of a colloidal suspension of polydisperse particles. Above a threshold c^* corresponding to the close packing of the vesicles, there is a second regime with the objects remaining at close packing. In the first step, vesicles shrink to accommodate the excess membrane added ; in the second step, freeze fracture pictures indicate that multilayered vesicles are formed. In our case it seems that, as the concentration of surfactant is increased even more (typically above 10 % in weight fraction) there is a first order transition to a lamellar phase. However, note that multilayered vesicles at close packing can be described as a molten lamellar phase with a smectic correlation length corresponding to the average size of the vesicles. In other words, if the vesicle size increases to infinity one can describe a continuous process towards a lamellar phase. From theoretical grounds it is however expected that this transition (isotropic to smectic) will remain first order [29]. One can also wonder why this phase is so narrow in the phase diagram in terms of alcohol concentration. It is known that the alcohol concentration tunes the Gaussian bending constant $\bar{\kappa}_0$ [30]. In fact this is nicely illustrated by the phase diagram itself that shows that, as the alcohol over surfactant ratio is increased, a phase of vesicles, a lamellar phase and a sponge phase are successively identified. One can expect that this corresponds to values of $\bar{\kappa}_0$ respectively negative, around zero and positive. Taking into account that κ in this system is rather large ($4 kT$) and that in order to stabilize vesicles $2 \kappa_0 + \bar{\kappa}_0$ has to be of the order of $k_B T$, this requires a fine tuning of $\bar{\kappa}_0$. we find $\bar{\kappa}_0 = - 3.4 kT$.

Acknowledgements.

We would like to thank J.-P. Derian and G. Guérin for helping us in preliminary experiments of viscosity measurements ; J.-C. Dedieu for skillful technical assistance in electron microscopy ; and O. Babagbeto for his praiseworthy help in preparing a whole wealth of samples.

Discussions with D. Andelman, B. D. Simons and specially M. E. Cates were extremely helpful in understanding our data.

We are grateful to S. T. Milner and D. Morse for their strong interest in evaluating vesicle entropy.

This work has been supported in part by Rhône-Poulenc.

Appendix.

Calculation of average quantities for vesicles in thermal equilibrium.

NOTATION :

N total number of surfactant molecules ;

$c = N v_s/V$ surfactant volume fraction (v_s is the surfactant volume, V the total volume) ;

n_i number of vesicles of size (aggregation number) i ; the radius r_i is related to i by :

$8 \pi r_i^2 = i \Sigma_s$, with Σ_s the area per surfactant molecule.

$n_{i,s} = i n_i$ number of surfactant in aggregates of size i ;

$X_i = c n_{i,s}/N$ volume fraction of surfactant in aggregates of size i ;

$\rho_i = c n_i/N$ volume fraction occupied by vesicles of size i .

According to equation (2) the elastic energy per vesicle is given by :

$$E_i = 4 \pi (2 \kappa_i + \bar{\kappa}_i). \quad (\text{A1})$$

Taking into account the effect of renormalization on the elastic bending constants, κ_i and $\bar{\kappa}_i$ are function of the radius r_i of the vesicles :

$$\kappa_i = \kappa_0 - \alpha \frac{k_B T}{4 \pi} \ln \left[\frac{r_i}{\delta} \right] \quad (\text{A2a})$$

$$\bar{\kappa}_i = \bar{\kappa}_0 + \bar{\alpha} \frac{k_B T}{4 \pi} \ln \left[\frac{r_i}{\delta} \right] \quad (\text{A2b})$$

with $\alpha = 3$ and $\bar{\alpha} = 10/3$.

The free energy of the aggregates of size i reads (neglecting vesicle-vesicle interactions) [31] :

$$F_i = n_i k_B T \ln [\rho_i] + n_i E_i \quad (\text{A3})$$

replacing n_i by the number of surfactant in aggregates of size i ($n_{i,s} = i n_i$) we get :

$$F_i = \frac{n_{i,s}}{i} k_B T \ln \left[\frac{X_i}{i^\gamma} \right] + \frac{n_{i,s}}{i} E_0 \quad (\text{A4})$$

with $\gamma = 1 + \alpha - \bar{\alpha}/2$.

In the literature there are some discrepancies in the values of the coefficients α and $\bar{\alpha}$ (respectively either 1,0 [22] or 3, 10/3 [23]) but this does not greatly affect the value of γ (2 or $7/3 \approx 2.33$ depending on the couple of values we keep). In what follows we will take the second values [23] :

$$\gamma = 7/3 .$$

The free energy of the ensemble of vesicles is given by the sum :

$$F = \sum_{i=1}^{i=\infty} F_i \quad (\text{A5})$$

minimizing this sum respecting the constraint :

$$c = \sum_{i=1}^{i=\infty} X_i \quad (\text{A6})$$

corresponds to a minimization of G :

$$G = \sum_{i=1}^{i=\infty} [F_i - \mu n_{i,s}] . \quad (\text{A7})$$

μ being a chemical potential the value of which allows equation (A6) to be fulfilled. The minimization is done respecting the distribution function $n_{i,s}$. We get the set of equations whatever i :

$$\mu = \frac{k_B T}{i} \ln \frac{X_i}{i^\gamma} + \frac{E_0}{i} \quad (\text{A8})$$

using the conservation of surfactant we get :

$$\sum_{i=1}^{i=\infty} X_i = c = \sum_{i=1}^{i=\infty} i^\gamma A^i e^{-\frac{E_0}{k_B T}} \quad (\text{A9})$$

with $A = X_1 \exp[E_0/k_B T]$

assuming A being very close to 1 (meaning that X_1 is close to the CVC value which can be checked *a posteriori*), we get equation (4) :

$$X_i = i^\gamma \left(1 - \left(\frac{\gamma! e^{-\frac{E_0}{kT}}}{c} \right)^{1/(\gamma+1)} \right)^i e^{-\frac{E_0}{kT}} \quad (\text{A10})$$

Using the same approximations we can calculate the average vesicle radius :

$$R = \frac{\sum_{i=1}^{i=\infty} n_i r_i}{\sum_{i=1}^{i=\infty} n_i} = r_0 \frac{(\gamma - 1/2)!}{(\gamma - 1)!} (\gamma!)^{\frac{1}{2(\gamma+1)}} (ac)^{\frac{1}{2(\gamma+1)}} \quad (\text{A11})$$

and the fraction of volume occupied by the vesicles :

$$\phi = \frac{\frac{4\pi}{3} \sum_{i=1}^{i=\infty} n_i r_i^3}{V} = \frac{r_0}{3\delta} \frac{(\gamma + 1/2)!}{(\gamma!)^{\frac{\gamma+1}{\gamma+3/2}}} (ac)^{\frac{1}{2(\gamma+1)}} c. \quad (\text{A12})$$

References

- [1] See Physics of Amphiphilic Layers, J. Meunier, D. Langevin and N. Boccaro Eds. (Springer Verlag, New York, Berlin, Heidelberg, 1987).
- [2] Roux D. and Bellocq A.-M., Physics of Amphiphiles : Micelles, Vesicles and Microemulsions, V. Degiorgio and M. Corti Eds. (North Holland, Amsterdam, 1985).
- [3] Porte G., Marignan J., Bassereau P. and May R., *J. Phys. France* **49** (1988) 511.
- [4] Cates, M. E., Roux D., Andelman D., Milner S. T. and Safran S., *Europhys. Lett.* **5** (1988) 733 ; erratum *ibid.* **7** (1988) 94.
- [5] a) Huse D. and Leibler S., *J. Phys. France* **49** (1988) 605 ;
b) Roux D., Coulon C. and Cates M. E., *J. Phys. Chem.* **96** (1992) 4174.
- [6] Gazeau D., Bellocq A.-M., Roux D. and Zemb T., *Europhys. Lett.* **9** (1989) 447.
- [7] Coulon C., Roux D. and Bellocq A.-M., *Phys. Rev. Lett.* **66** (1991) 1709.
- [8] Brady J. E., Evans D. F., Kachar B. and Ninham B. W., *J. Amer. Chem. Soc.* **106** (1984) 4279.
- [9] a) Schurtenberger P. and Hauser H., *Biochim. Biophys. Acta* **778** (1984) 470 ;
b) Hauser H., Gains N., Eibl H. J., Muller M. and Wehrli, *Biochemistry* **24** (1986) 2126.
- [10] Thunig C., Platz G. and Hoffman H., unpublished.
- [11] Hauser H., Gains N. and Lasic D. D., Physics of Amphiphiles : Micelles, Vesicles and Microemulsions, V. Degiorgio and M. Corti Eds. (North Holland, Amsterdam, 1985).
- [12] Kaler E. W., Murthy K. A., Rodriguez B. E. and Zasadzinski J. A. N., *Science* **245** (1989) 1371.
- [13] Cantu L., Corti M., Musolino M. and Salina P., *Europhys. Lett.* **13** (1990) 561.

- [14] Israelachvili J., *Physics of Amphiphiles : Micelles, Vesicles and Microemulsions*, V. Degiorgio and M. Corti Eds. (North Holland, Amsterdam, 1985).
- [15] Safran S., Pincus F. and Andelman D., *Science* **248** (1990) 354.
- [16] Hervé P., Bellocq A.-M., Roux D. and Nallet F., unpublished.
- [17] Shinoda K., *Colloid Surfactants, Some Physicochemical Properties* (Acad. Press, 1963).
- [18] Anderson D. M. and Wennerström H., *J. Phys. Chem.* **94** (1990) 8683.
- [19] Auguste F., Bellocq A.-M., Roux D., Nallet F. and Gulik T., unpublished.
- [20] In fact, careful measurements show that a slight deviation, specially for the very dilute systems can be observed. Such a deviation might come from the polydispersity.
- [21] Helfrich W., *Z. Naturforsch.* **28c** (1973) 693.
- [22] Helfrich W., *J. Phys. France* **46** (1985) 1263.
- [23] Peliti L. and Leibler S., *Phys. Rev. Lett.* **54** (1986) 1690.
- [24] Helfrich W., *J. Phys. France* **47** (1986) 321.
- [25] Jonsson B., Wennerström H., Nilsson P. G. and Linse P., *Colloid Polym. Sci.* **264** (1986) 77.
- [26] a) DiMeglio J.-M., Dvolaitzky M. and Taupin C., *J. Phys. Chem.* **89** (1985) 871 ;
b) Safinya C. R., Sirota E. B., Roux D. and Smith G. S., *Phys. Rev. Lett.* **62** (1989) 1134 ;
c) Szleifer I., Kramer D., Ben-Shaul A., Roux D. and Gelbart W. M., *Phys. Rev. Lett.* **60** (1988) 1966.
- [27] De Kruijff C. G., van Iersel E. M. F., Vrij A. and Russel W. B., *J. Chem. Phys.* **83** (1986) 4717.
- [28] Simons B. D. and Cates M. E., *J. Phys. II France* **2** (1992) 1439.
- [29] Brazovskii S., *Sov. Phys. JETP* **41** (1976) 91.
- [30] Porte G., Appell J., Bassereau P. and Malignan J., *J. Phys. France* **50** (1989) 1335.
- [31] Subtle problems arise in evaluating correctly the entropy for a *polydisperse* assembly of *rotating* and *fluctuating* vesicles. In the model detailed here, we do not take into account the size dependence of the translational or rotational contributions to the entropy, for instance, nor the entropy content of the shape fluctuations. This may change the value of γ .
- [32] Rigault J.-P., *Micron Microscopica Acta* **15** (1984) 1.